


# Genetic screening and functional analysis of *CASP9* mutations in a Chinese cohort with neural tube defects

Xiao-Zhen Liu<sup>1,2</sup> | Qin Zhang<sup>1</sup> | Qian Jiang<sup>1</sup> | Bao-Ling Bai<sup>1</sup> | Xiao-Juan Du<sup>3</sup> | Fang Wang<sup>1</sup> | Li-Hua Wu<sup>1</sup> | Xiao-Lin Lu<sup>1</sup> | Yi-Hua Bao<sup>1</sup> | Hui-Li Li<sup>1</sup> | Ting Zhang<sup>1,2</sup> 

<sup>1</sup>Beijing Municipal Key Laboratory of Child Development and Nutriomics, Capital Institute of Pediatrics, Beijing, China

<sup>2</sup>Graduate School, Peking Union Medical College, Beijing, China

<sup>3</sup>Department of Cell Biology, School of Basic Medical Sciences, Peking University Health Science Center, Beijing, China

## Correspondence

Ting Zhang, Beijing Municipal Key Laboratory of Child Development and Nutriomics, Capital Institute of Pediatrics, Beijing, China.  
Email: zhangtingcv@126.com  
and

Hui-Li Li, Beijing Municipal Key Laboratory of Child Development and Nutriomics, Capital Institute of Pediatrics, Beijing, China.  
Email: lihuli2011@gmail.com

## Funding information

National Natural Science Foundation of China, Grant/Award Number: 81471163, 81701441 and 81771584; National Science & Technology Pillar Program, Grant/Award Number: 2013BA112B00; CAMS Initiative for Innovative Medicine, Grant/Award Number: CAMS-I2M-1-008

## Summary

**Aim:** Neural tube defects (NTDs) are birth defects of the nervous system and are the second most frequent cause of birth defects worldwide. The etiology of NTDs is complicated and involves both genetic and environmental factors. *CASP9* is an initiator caspase in the intrinsic apoptosis pathway, which in *Casp9*<sup>-/-</sup> mice has been shown to result in NTDs because of decreased apoptosis. The aim of this study was to evaluate the potential genetic contribution of the *CASP9* gene in human NTDs.

**Methods:** High-throughput sequencing was performed to screen genetic variants of *CASP9* genes in 355 NTD cases and 225 matched controls. Apoptosis-relevant assays were performed on transiently transfected E9 neuroepithelial cells or human embryonic kidney 293T cells, to determine the functional characteristics of NTD-specific rare variants under complete or low folic acid (FA) status.

**Results:** We found significant expression of *CASP9* rare variants in NTDs and identified 4 NTD-specific missense variants. Functional assays demonstrated that a p.Y251C variant attenuates apoptosis by reducing *CASP9* protein expression and decreasing activity of the intrinsic apoptosis pathway. From this, we conclude that this variant may represent a loss-of-function mutation. A 4-time recurrent p.R191G variant did not affect intrinsic apoptosis in complete medium, while it completely inhibited apoptosis induced by low FA medium.

**Conclusion:** Our findings identify a genetic link for apoptosis in human NTDs and highlight the effect of gene-environment interactions in a complex disease.

## KEYWORDS

apoptosis, *CASP9*, human, mutation, neural tube defects

## 1 | INTRODUCTION

Neural tube defects (NTDs) are a group of severe birth defects of the central nervous system, which are caused by failure of neural tube closure (NTC) during embryogenesis. NTDs are the second most common birth defect in the world, affecting 0.5-2 live births per 1000, with varying prevalence in different populations.<sup>1</sup> NTDs are categorized according to their clinical phenotypes: anencephaly (cranial region), encephalocele (cranial region), spina bifida (spinal region), and

craniorachischisis (in which along from the brain to the low spinal cord may be open). Spina bifida is the only form of NTDs that is not fatal; however, these individuals generally suffer from lifelong disabilities.<sup>2</sup>

The etiology of NTDs is complicated and involves both genetic and environmental factors. Epidemiological studies have revealed that folate deficiency may increase the risk of NTDs in humans, and that folic acid (FA) supplementation during periconception can reduce this risk.<sup>3-6</sup> Although the genetic causation of human NTDs is poorly understood, studies in more than 240 mutant mouse models of NTDs

provide the basis for a plausible pathological mechanism. In addition to null, hypomorphic, and conditional mutations of candidate genes in animal models of NTDs, point mutations can also lead to NTD phenotypes,<sup>7</sup> suggesting a possible contribution for rare variants in the etiology of human NTDs. NTC is a dynamic process in which the neural plate elevates, bends, and fuses to shape the neural tube. Therefore, the process of cell apoptosis in the correct balance is necessary for normal neural tube development.<sup>8</sup> Excessive apoptosis results in a lack of available cells for the formation of the neural tube; this is one of the most common phenotypes observed in animal models.<sup>9,10</sup> However, live imaging studies in cultured mouse embryos have also shown that inhibition of apoptosis can increase the risk of exencephaly.<sup>8</sup>

Caspases, the main components of the apoptotic process, are a group of proteases with essential cysteine residues in the active site that are required for substrate cleavage.<sup>11</sup> Caspase-9, originally discovered in *Caenorhabditis elegans*, is the initiator caspase of the intrinsic apoptosis pathway. This caspase functions with cytochrome *c* and apoptotic protease-activating factor-1 (APAF-1) to activate executioner caspase-3, subsequently triggering activation of the caspase cascade.<sup>12</sup> *Casp9* deficiency in the 129/SvJ mouse results in abnormalities, including exencephaly in the mid- and hindbrain, and enlarged ventricular zones in the fore- and midbrain.<sup>13-16</sup> Similarly, a lack of *Apaf-1*, *Casp3*, or *cytochrome c* causes ventricular zone expansion, brain overgrowth, and exencephaly,<sup>17-20</sup> suggesting that this cascade is crucial for cranial NTC. Interestingly, a polymorphic genotype, *CASP9* c.1263A>G, reduces predisposition for the risk of bladder, gastric, and colorectal cancer, while increasing the risk of lung cancer.<sup>21-24</sup> This suggests that a genetic variant of the *CASP9* gene contributes to human disease, but the impact on function can be diverse depending on the context.

The crucial role of *Casp9* gene in mouse models of NTC, and the genetic impact of the *CASP9* gene in human cancers, prompted us to investigate the effects of *CASP9* variants in human NTDs. After screening exonic regions and highly conserved regions of the *CASP9* gene in 355 individuals with NTDs and 225 controls, we identified significant expression of rare variants in the present NTD cohort. Apoptosis-relevant functional assays demonstrated that the missense mutation (p.Y251C) is a loss-of-function variant; furthermore, the missense mutation (p.R191G) results in a loss of the apoptotic response in low FA settings.

## 2 | MATERIALS AND METHODS

### 2.1 | Human subjects

This study recruited 355 Chinese Han individuals with sporadic NTDs, collected from multiple locations in the Shanxi, Tianjin, Jiangsu, Liaoning, and Heilongjiang provinces between 2005 and 2011. Clinical pathologists diagnosed all patients with NTDs. A total of 225 NTD-unrelated ethnicity- and geography-matched subjects were recruited as controls. The parents of all subjects provided written informed consent, according to the requirements of the Medical Ethics Committee of Capital Institute of Pediatrics (Beijing, China). All studies

were conducted in accordance with the principles of the Declaration of Helsinki.

### 2.2 | Genomic DNA sequencing

Genomic DNA was extracted from the human subjects using the Blood and Tissue DNA Kit (Qiagen). DNA was fragmented and enriched for coding regions and highly conserved regions in the *CASP9* gene. Samples were then prepared using a Truseq Sample preparation kit (Illumina), following the manufacturer's standard protocol. The library was constructed with an Agilent Custom SureSelect Enrichment Kit (Agilent Technologies) and an Agilent Custom Enrichment array. The hybridization reactions were carried out on an AB 2720 Thermal Cycler (Life Technologies Corporation). Reacted samples were incubated in a hybridization mixture for 24 hours at 65°C with a heated lid at 105°C. Custom capture oligonucleotides were designed using the SureDesign Web site of Agilent Technologies. The capture production was enriched with the following cycling conditions: 98°C for 30 seconds; 10 cycles of 98°C for 10 seconds; 60°C for 30 seconds; 72°C for 30 seconds, and 72°C for 5 minutes. Base incorporation then was carried out on a Genomic Analyzer II Sequencer (Illumina) following the manufacturer's standard sequencing protocols. The sequencing reads were aligned to the UCSC GRCh37/hg19 of the reference human genome using the Burrows-Wheeler Aligner v6.4. Polymerase chain reaction (PCR) repeated sequences were sorted and removed using Picard software. Single nucleotide variant (SNV) calling was carried out using the Genome Analysis Toolkit (GATK) and VarScan, and SNVs then were annotated with ANNOVAR. Genotype calling was performed using BayesAss 3.03, and the identified variants were filtered using dbSNP and the Genome 1000 browser, to identify shared variants in the cases and controls. Sanger sequencing was performed to trace the missense mutations.

### 2.3 | Plasmids, cell culture, and transfection

Wild-type (WT) human *CASP9* and variant open-reading frames (ORFs), labeled with the Myc-DDK tag at their C-termini, were synthesized by OriGene Technologies and cloned into the expression vector pCMV6-AC. All WT and variant plasmids were validated by direct DNA sequencing. NE-4C cells, purchased from the Stem Cell Bank, Chinese Academy of Science, were cultured on 10-cm<sup>2</sup> cell culture dishes coated with 10 g/mL Poly-D-Lysine (Millipore), and grown in Eagle's minimal essential medium (MEM) (ThermoFisher). HEK293T cells were cultured in Dulbecco's modified Eagle's medium (DMEM) (ThermoFisher). To investigate changes in the mutants in response to FA deficiency, we cultured HEK293T cells for 72 hours in low FA medium (DMEM-low glucose (Sigma), supplemented with 3.7 g/L sodium bicarbonate, 0.584 g/L L-glutamine, 3.5 g/L glucose, and sterile distilled water). All media were supplemented with 10% fetal bovine serum (FBS) (ThermoFisher), 1% antibiotic, 1% GlutaMAX (Invitrogen), and 1% nonessential amino acids (Invitrogen). In the DMEM, the folate concentration was 9.0 μmol/L, and in the low FA DMEM, the folate concentration was 1.5 nmol/L.<sup>25</sup> Once the cells covered 80% of

the 10-cm<sup>2</sup> cell culture dishes, they were passaged into 4 10-cm<sup>2</sup> cell culture dishes. After 24 hours, the cells were transiently transfected with 4 µg of WT or variant *CASP9* plasmid using Lipofectamine 2000 (Invitrogen). Cotransfection with 0.5 µg of a green fluorescent protein (GFP)-expression plasmid was used to evaluate the transfection efficiency. To investigate changes in the variants in response to ultraviolet (UV) radiation, we exposed the HEK293T cells to UV irradiation (80 mJ/cm<sup>2</sup>) using the DNA Stratalinker, 20 hours after transiently transfecting the cells. Cells were then sequentially cultured in DMEM for 24 hours.

## 2.4 | Western blotting

Cells were harvested at 24 or 48 hours after transfection and lysed in EBC250 buffer<sup>26</sup> for 10 minutes. An equal amount of total lysate proteins were separated by 8%-12% sodium dodecyl sulfate-polyacrylamide gel electrophoresis (SDS-PAGE) and then transferred to a polyvinylidene fluoride (PVDF) membrane (Amersham Biosciences). Specific antibodies were purchased from Cell Signaling Technology: Caspase-9 (#9502) and PARP (#9532); from Abcam: Caspase-3 (ab32351); from Merck Millipore: Myc (16-212); from Santa Cruz Biotechnology: Actin (sc-1516); and from OriGene: GFP (TA15002). Immunocomplexes were detected with the ECL kit (GE Healthcare). Bands were quantified using the gray density of each band, the data were standardized to the Actin band, and then the data were normalized to corresponding WT band.

## 2.5 | CASP9 and CASP3 activity assays

The activities of CASP9 and CASP3 were tested using CASP9 and CASP3 activity kits (Beyotime Institute of Biotechnology). Following previously described treatments, the NE-4C and HEK293T cells were collected. The admixture included 10 µL of whole-cell protein lysate, 80 µL of reaction buffer, 10 µL of CASP9 substrate acetyl-Leu-Glu-His-Asp *p*-nitroaniline (Ac-LEHD-*p*NA, 2 mmol/L), or CASP3 substrate acetyl-Asp-Glu-Val-Asp *p*-nitroaniline (Ac-DEVD-*p*NA, 2 mmol/L). This was maintained in an incubator at 37°C for 20 hours and then measured via enzyme-linked immunosorbent assay (ELISA) at an absorbance of 405 nm. CASP9 and CASP3 activities were calculated based on a standard curve. These experimental processes were performed according to the manufacturer's instructions.

## 2.6 | Real-time quantitative PCR

HEK293T cells were transfected with WT or mutant *CASP9* plasmids and harvested at 24 hours after transfection. Total RNA was isolated using the Trizol reagent (Invitrogen), and *CASP9* mRNA expression was analyzed using an ABI 7500 Fast Real-Time PCR system (Applied Biosystems). Human *ACTB* was used as a reference gene. The primers were as follows: *CASP9* forward, 5-AGGTTCTCAGACCGGAAACA-3, and reverse, 5-CTGCATTTCCCTCAAATC-3; *ACTB* forward, 5-ATGGGTGAGAAGGATTCCTATGT-3, and reverse, 5-AAGGTCTCAAACATGATCTGGG-3. All expression values were represented by the

cycle threshold (Ct) value, standardized by *ACTB*, and then normalized to WT.

## 2.7 | Annexin-V and propidium iodide (PI) assays

To investigate the role of the mutants in the apoptosis of HEK293T cells, we counted apoptotic cells under complete and low FA culture conditions. Following treatment, cells were digested by trypsin without EDTA, washed with cold PBS, and double stained with annexin-V and PI (KeyGen). Flow cytometry analysis was performed using green fluorescent fluorescein isothiocyanate (FITC) channel tests for annexin-V, and red fluorescent for PI. The percentage of apoptotic cells was determined for 10 000 cells.

## 2.8 | Tissue folate concentration determination

Brain tissues were collected, and the folate levels were determined using a competitive receptor binding immunoassay (Chemiluminescent Immunoenzyme Assay; Beckman Coulter). The folate concentration was analyzed, and readout was accomplished using the Access 2 Immunoassay system (Beckman Coulter). The detailed experimental processes were performed according to the manufacturer's instructions.

## 2.9 | Statistical analysis

In the variation rate analysis of human subjects, difference between cases and controls was evaluated by Chi-squared test, or Fisher's exact test. In the cellular experiments, statistical significance was evaluated using one-way analysis of variance (ANOVA). All results are expressed as mean ± SD. All reported *P* values are 2-sided, and *P* < 0.05 was considered statistically significant. All data statistical analysis was performed using SPSS 20.0 software.

# 3 | RESULTS

## 3.1 | Rare variants identified in the *CASP9* gene

In 29 NTDs cases, 20 mutations were identified whereas 8 mutations were found in 8 controls (Table 1, *P* = 0.027), suggesting that NTDs cases carry more *CASP9* mutations than controls. The minor allele frequency was < 1%, and all rare variants were heterozygous.

## 3.2 | Rare missense variants in *CASP9* gene in NTDs

Among the variants, p.G66A (c.197G>C), p.R173C (c.517C>T, rs372045782), p.R191G (c.571C>G), and p.Y251C (c.752A>G, rs552167727) were missense variants identified in NTD cases; they were absent in controls. The p.R173C, p.R191G, and p.Y251C variants were reported in either the ESP database (<http://evs.gs.washington.edu/EVS/>) or the ExAC database (<http://exac.broadinstitute.org/>); however, the p.G66A is a novel mutation. The p.R191G variant occurred in 4 patients. Clinical data of missense

**TABLE 1** Summary of *CASP9* gene rare variants identified in a Chinese population

	Number of individual in NTDs (355)	Number of individual in controls (225)	P value (NTDs vs controls)
Missense rare variants	7 <sup>a</sup>	1	0.124 <sup>e</sup>
Silent rare variants	1	1	0.626 <sup>f</sup>
Rare variants in the intronic region	13 <sup>b</sup>	6	0.512 <sup>e</sup>
Rare variants in the upstream	5 <sup>c</sup>	0	0.073 <sup>e</sup>
Rare variants in the 5'UTR region	3 <sup>d</sup>	0	0.167 <sup>e</sup>
Total	29	8	0.027 <sup>e</sup>

<sup>a</sup>One of the missense variants is a recurrent variation and was carried by 4 individuals.

<sup>b</sup>Three of the variants in the intronic region are recurrent variations and were carried by 2 individuals.

<sup>c</sup>One of the variants in the upstream region is a recurrent variation and was carried by 3 individuals.

<sup>d</sup>One of the variants in the 5'UTR region is a recurrent variation and was carried by 2 individuals.

<sup>e</sup>P value was calculated by Chi-squared test.

<sup>f</sup>P value was calculated by Fisher's exact test.

**TABLE 2** Clinical characteristics of *CASP9* missense variants in affected NTDs cases

Missense variant	Patient ID	Gender	Gestational weeks	Clinical phenotypes	Folate concentration (ng/mg)
p.G66A	A1469	Female	14	Anencephaly, parietal meningoencephalocele, absence of neck, atelectasis, chest pericardial cavity small hemorrhagic effusion	NA
p.R173C	A2195	Female	27	Anencephaly, occipital cervical spinal bifida aperta, short neck, bilateral adrenal hypotrophy, thymus hypertrophy, visceral congestion	NA
p.R191G	A1586	Male	25	Hydrocephalus, lumbosacral spina bifida aperta, left leg short deformity, bilateral atelectasis, intracranial hemorrhage, visceral congestion	0.089
	A2225	Male	24	Hydrocephalus, whole spinal bifida aperta, bilateral polycystic kidney, bilateral adrenal dysplasia, bilateral atelectasis, visceral congestion	0.1125
	A2322	Female	24	Hydrocephalus, thoracic spina bifida cystica, lung lobe branching malformation, bilateral atelectasis, visceral congestion	NA
	A2761	Male	22	Hydrocephalus, lumbosacral spina bifida cystica, bilateral atelectasis, visceral congestion	0.1965
p.Y251C	A1938	Male	21	Hydrocephalus, lumbosacral spina bifida aperta, talipes equinovarus, right lung lobe deformity, left renal pelvis moderate expansion, thoracic and abdominal pericardial cavity of hemorrhagic effusion, visceral congestion	0.0567

NA, not available.

*CASP9* protein reference sequence NP\_001220.2.

variant-affected patients are shown in Table 2. The p.G66A was located in the caspase activation and recruitment domain (CARD), an APAF-1 interaction motif of *CASP9*. Other variants (p.R173C, p.R191G, and p.Y251C) were located in the caspase domain, which forms the substrate-binding groove and contains the catalytic residue cysteine (Figure 1A,B).<sup>27</sup> Amino acid conservation analysis showed that the p.G66A and p.Y251C mutations affected highly conserved amino acid residues, while p.R173C and p.R191G mutations affected poorly conserved amino acid residues (Figure 1C and

Table 3). Functional prediction analysis showed that p.G66A and p.R191G were likely to be damaged by SIFT, and p.G66A, p.R173C, and p.Y251C were likely to be damaged by PolyPhen (Table 3). The p.K292E (c.874A>C) was a missense variant identified in controls (Figure 1A,B). In view of the frequency of recurrence, genomic location, conservation, and bioinformatics analysis, we focused on the 3 NTD-specific missense mutations (p.G66A, p.R191G, and p.Y251C) in the following experiments. These mutations were traced via Sanger sequencing (Figure 1C).

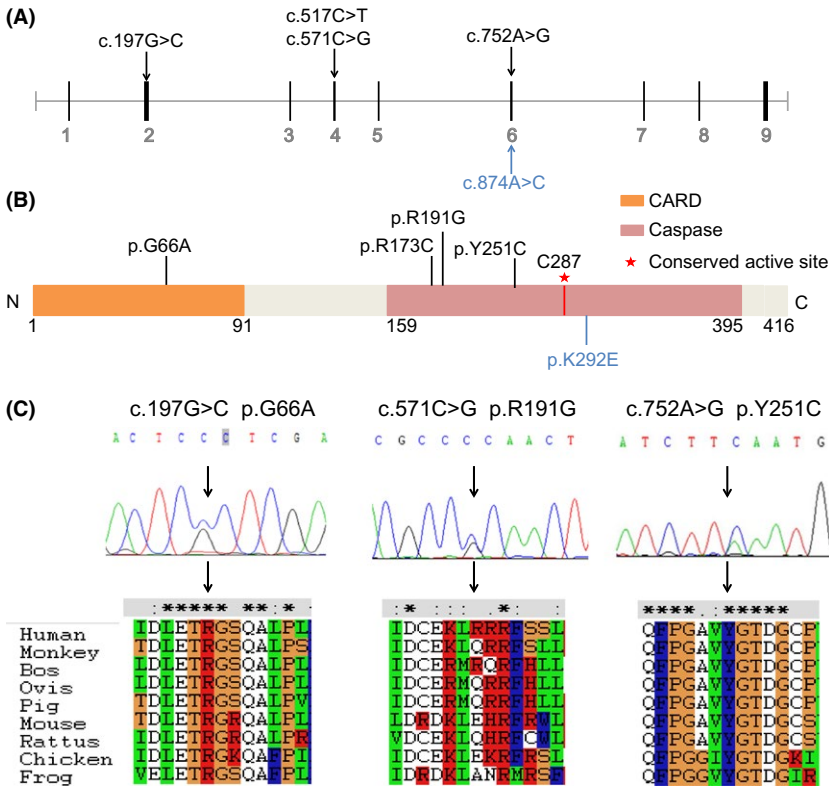


**FIGURE 1** Rare missense variants identified in the CASP9 gene. (A), (B) Structure of the CASP9 transcript (NM\_001229.3) and protein (NP\_001220.2), and positions of the identified missense variants in the present cohort. Variations in NTD cases are represented by black arrows, and variations in the controls are represented by blue arrows. (C) Heterozygous variations traced via sequencing chromatograms; changes in the transcript and protein sequence are depicted. Alignment of human CASP9 protein sequence with other orthologous sequences using ClustalW. Solid black arrows indicate a variation. The orthologous sequences include: Monkey, XP\_001082859.1; Cow, NP\_001192433.1; Sheep, XP\_014954788.1; Pig, XP\_013854451.1; Mouse, NP\_056548.2; Rat, NP\_113820.1; Chicken, XP\_424580.5; and Frog, NP\_001079035.1

**TABLE 3** Analysis of amino acid substitutions in missense variants of neural tube defects (NTDs) cases

Missense variant	Conservation <sup>a</sup>	Class change <sup>b</sup>	Property change <sup>c</sup>	SIFT <sup>d</sup>	PolyPhen 2 <sup>e</sup>		
p.G66A	Yes	Aliphatic-aliphatic	Polar (neutral)—nonpolar (neutral)	Damaging	0	Probably damaging	1
p.R173C	No	Aliphatic-aliphatic	Polar (positive)—polar (neutral)	Tolerated	0.081	Probably damaging	0.991
p.R191G	No	Aliphatic-aliphatic	Polar (positive)—polar (neutral)	Damaging	0.022	Benign	0.185
p.Y251C	Yes	Aromatic-aliphatic	Polar (neutral)—polar (neutral)	Tolerated	0.067	Possibly damaging	0.612

<sup>a</sup>Amino acid residue evolutionary conservation.

<sup>b</sup>Amino acid residue class change.

<sup>c</sup>Amino acid residue property change.

<sup>d</sup>Score ranges from 0 to 1; the amino acid substitution was predicted to be damaging if the score was  $\leq 0.05$  and tolerated if the score was  $>0.05$ , prediction cutoff = 0.05.

<sup>e</sup>Score ranges from 0 to 1; the amino acid substitution was assessed for whether it was damaging according to the false-positive rate.

### 3.3 | The p.Y251C variant-affected protein expression and CASP9 activity

Given that CASP9 is a cysteine-containing aspartate-specific protease, we addressed the question of whether the 3 rare missense variants affected protease activity. WT CASP9 and mutant plasmids tagged with Myc were constructed and transiently transfected into NE-4C cells, which is a rodent p53-deficient E9 neural ectoderm cell line.<sup>28,29</sup> Because p53 plays a role upstream of CASP9 during the apoptosis process, it would be advantageous for NE-4C cells to avoid the biological impacts of p53. Western blotting assays revealed that protein levels of CASP9-tagged-Myc

and pro-CASP9 in the p.Y251C variant were significantly lower than those in WT (Figure 2A); this result was confirmed in another human embryonic cell line, HEK293T (Figure 2B). Cleaved-CASP9 (the active form) was consistently decreased in the p.Y251C variant (Figure 2A,B). In addition, CASP9 activity in both NE-4C and HEK293T cells was 0.35- and 0.5-fold lower, respectively, than in the WT cells ( $P < 0.05$ ), in contrast, CASP9 activity in the other 2 mutants was similar to the WT (Figure 2C,D). CASP9 mRNA levels in these variants were comparable to the levels in WT (Figure 2E), suggesting that protein stability of the p.Y251C variant may be impaired, and consequently, this may lead to a reduction in total CASP9 activity.

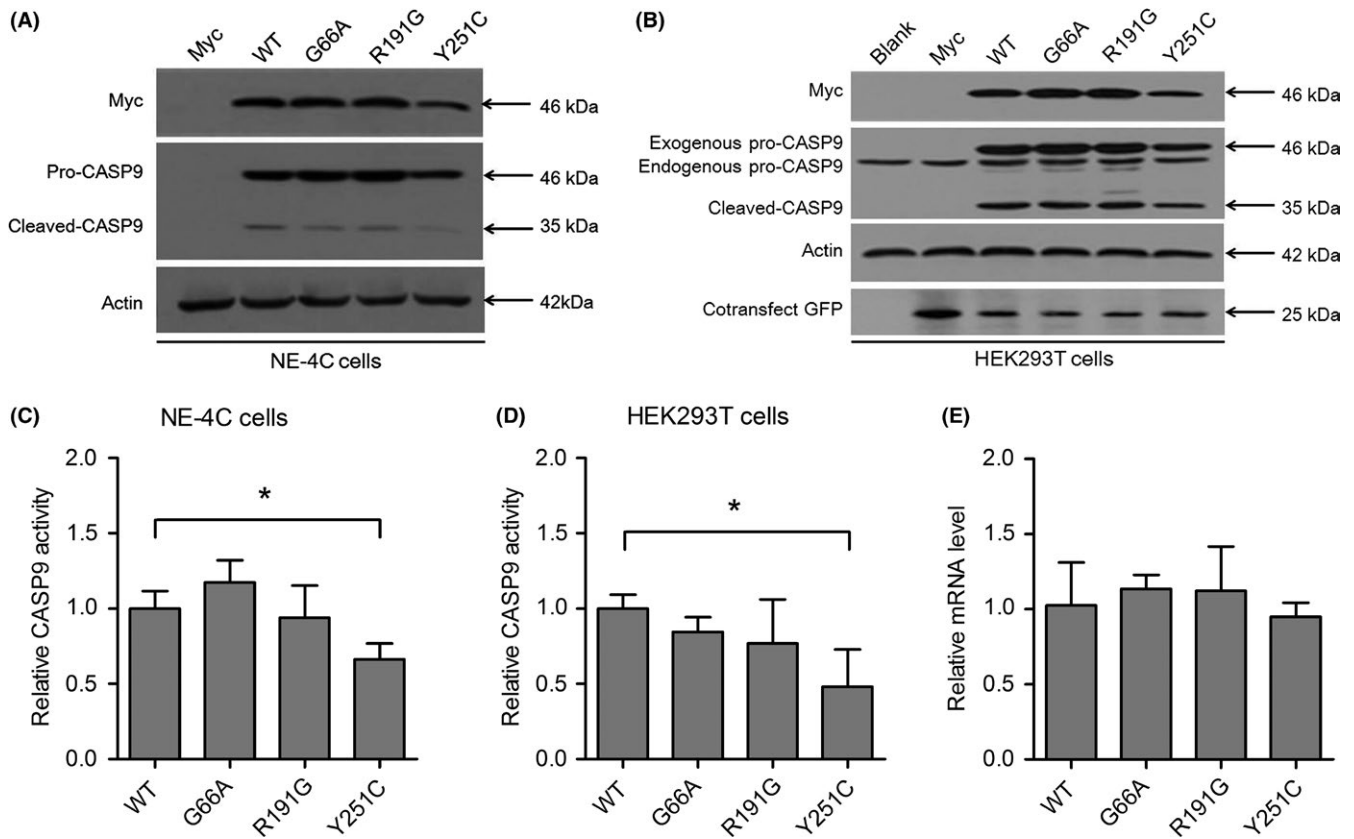


**FIGURE 2** Effects of *CASP9* missense variations on *CASP9* protein expression and activity. (A) NE-4C cells and (B) HEK293T cells were transfected with Myc-wild-type (WT), Myc-mutant, or Myc vector plasmid. Western blotting was performed with whole-cell protein lysate and analyzed proteins were immunoblotted with anti-Myc antibody (upper) and anti-CASP9 antibody (lower) ( $n = 3$  for each group).  $\beta$ -actin served as a loading control. (B) GFP transfection efficiency control in HEK293T cells. (C) *CASP9* protease activity in transfected NE-4C cells using consumption of the reaction substrate in cell lysates containing either mutant or WT ( $n = 3$ ). (D) *CASP9* activity in transfected HEK293T cells, measured as in (C) ( $n = 3$ ). (E) *CASP9* mRNA levels in WT or mutants in transfected HEK293T cells; the *ACTB* gene was used as a control. The average value of WT in 3 independent experiments was set to 1, and each value in other groups was normalized to this. Data are mean  $\pm$  SD, \* $P < 0.05$

### 3.4 | The p.Y251C variant impaired apoptotic function

As an initiator caspase of the apoptosis signaling pathway, *CASP9* can activate downstream executioner caspases, which involves cleavage of the signaling molecules executioner *CASP3*, and the apoptotic substrate *PARP*. *CASP3* and *PARP* levels are an indirect indication of the status of *CASP9* activity.<sup>12</sup> In the p.Y251C variant, we found that the levels of cleaved-*CASP3* and cleaved-*PARP* were significantly attenuated compared with WT ( $P < 0.05$ ; Figure 3A); proprotein levels were not altered. Furthermore, *CASP3* activity in the p.Y251C variant was significantly reduced by 0.4-fold in HEK293T cells ( $P < 0.05$ ; Figure 3B). To further test the possible impairment of apoptosis at the cellular level, we then performed annexin-V and PI assays in HEK293T cells. Consistent with the *CASP9* and *CASP3* activities, the percentage of apoptotic cells in the p.Y251C variant decreased by 0.5-fold compared with the WT ( $P < 0.05$ ; Figure 3C). Taken together, our cell-based assays demonstrated that the p.Y251C variant affects apoptotic function and suggested that this might be a loss-of-function variant.

### 3.5 | The p.R191G and p.Y251C variants inhibited low (FA)-induced apoptosis

Given epidemiological studies indicate low maternal serum folate levels in the present NTDs cohort,<sup>30</sup> we therefore assayed the local folate concentrations in brain tissues of the NTD cases with *CASP9* rare missense variants and matched controls ( $n = 104$ ). Our data showed that brain tissue folate concentrations were  $0.138 \pm 0.003$  ng/mg in controls. In our previous study, the fetal brain tissue folate concentration in 51 controls was  $0.136 \pm 0.005$  ng/mg,<sup>5</sup> which is similar to our present result. Importantly, in the NTD cases A1586 and A1938, the folate levels were 0.089 and 0.0567 ng/mg, respectively, clearly lower than controls (Table 2). This suggests that folate insufficiency might be an environmental factor in cases carrying the *CASP9* rare variants.

To understand the possible interplay of low folate levels and missense mutations, we performed apoptotic function assays in HEK293T cells cultured under low FA condition. After 48 hours of culturing in low FA medium, cells were transfected with the mutants or WT plasmid and grown in the same medium for 24 hours before harvesting. The results indicated that low FA culturing increased

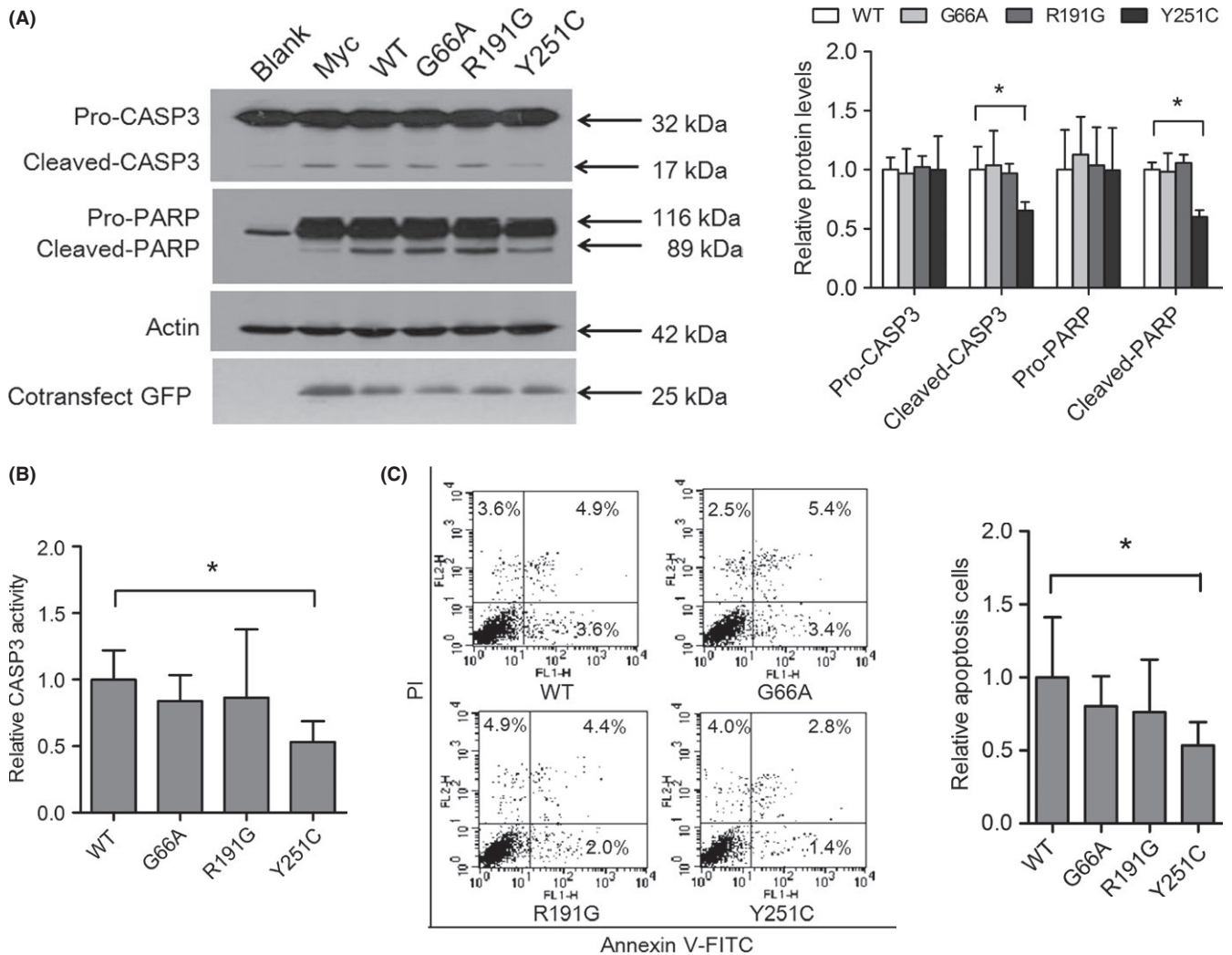


**FIGURE 3** The p.Y251C variant impaired apoptotic function. In transfected HEK293T cells, (A) Western blotting was performed with whole-cell protein lysate using anti-CASP3 antibody (upper) and anti-PARP antibody (lower) ( $n = 3$ ). GFP served as a transfection efficiency control, and  $\beta$ -actin served as a loading control. A representative result is shown in the left panel. The right panel represents relative protein levels of CASP3 and PARP. (B) CASP3 protease activity was measured using the consumption of the reaction substrate in cell lysates containing either mutant or WT ( $n = 3$ ). (C) Cell apoptosis was analyzed by flow cytometry after double staining with annexin-V fluorescein isothiocyanate (FITC) and propidium iodide (PI) ( $n = 5$ ). A representative result is shown in the left panel. The quantitative data of relative apoptotic cell levels are in the right panel. The average value of WT in independent repeated experiments was set to 1, and each value was normalized to the WT. Data are mean  $\pm$  SD, \* $P < 0.05$

protein expression of CASP9 and PARP, protease activities of CASP9 and CASP3, and the percentage of apoptotic cells in WT (Figure 4A–D). These results are consistent with a previous report, in which local low FA concentrations promoted apoptosis. However, in the p.R191G mutant, although the expression levels of pro-CASP9 and Myc-tagged CASP9 mildly increased compared with those in complete medium, there was no significant change in cleaved-CASP9, pro-PARP, and cleaved-PARP levels compared with those in complete medium (Figure 4A). Moreover, although the CASP9 activity was slightly higher (Figure 4B), CASP3 activity and numbers of apoptotic cells in the p.R191G variant were not different from those of WT cultured in complete medium (Figure 4C,D), suggesting that unlike in the WT, apoptosis induced by low FA levels is blocked in the p.R191G variant. To understand whether the p.R191G variant is unique resistant to low FA levels, we examined CASP9 activity in

transfected HEK293T cells treated with UV radiation (80 mj/cm<sup>2</sup>). By contrast to response to low FA, with UV treatment, the CASP9 protease activity in the p.R191G variant was dramatically increased and was similar to the WT (Figure 4E). Additionally, compared with that of WT, the apoptotic levels of p.Y251C variant decreased in low FA culture medium as well, as if in complete culture medium (Figure 4B–D). The apoptotic cell percentage in the p.Y251C variant under low FA medium was no significant change from in the WT under complete medium (Figure 4D).

## 4 | DISCUSSION

Results of animal studies support the hypothesis that Casp9 plays a role in NTC: (i) a null mutation of *Casp9* causes fetal mouse brain

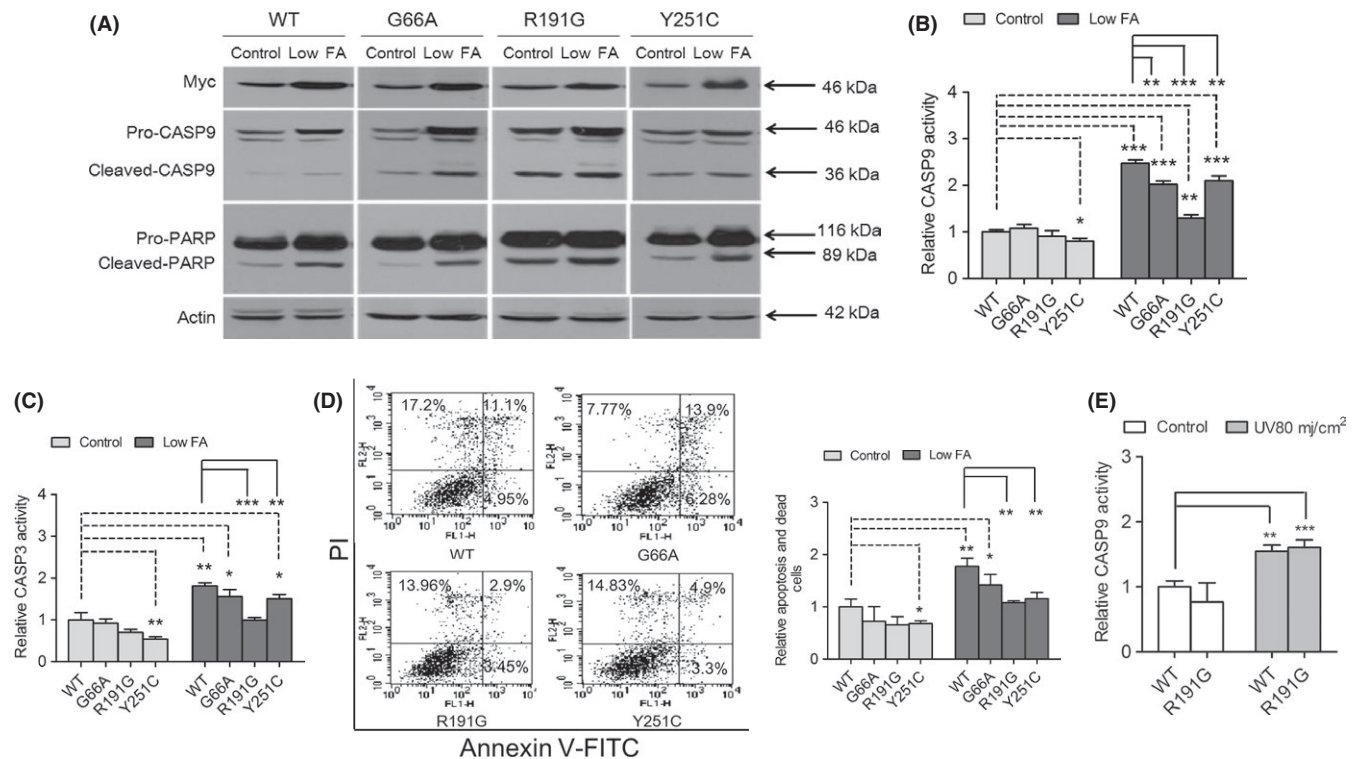


**FIGURE 4** The p.R191G and p.Y251C inhibited apoptosis in low folic acid (FA) condition. Transfected HEK293T cells were cultured in low FA medium. Western blotting results (A), CASP9 activity (B), CASP3 activity (C), and apoptosis (D) indicate changes in the mutants under low FA culture. (E) HEK293T cells transfected with either WT or the p.R191G variant were treated with 80 mJ/cm<sup>2</sup> UV radiation. Twenty-four hours later, cells were harvested for CASP9 activity measurement. Data are representative of 3 different experiments. The average value of control WT in independently repeated experiments was set to 1, and each value was normalized to control WT. Data are mean  $\pm$  SD, \* $P$  < 0.05, \*\* $P$  < 0.01, and \*\*\* $P$  < 0.001

malformations, including mid-hindbrain exencephaly, forebrain protrusion, and ventricle compression<sup>13,15</sup>; (ii) apoptotic cells have been observed in the neurulation stage during NTC in both vertebrate and invertebrate embryos, particularly in the boundary region, and inhibiting apoptosis delays the cranial NTC process<sup>8,31</sup>; and (iii) deficiency of other intrinsic apoptotic pathway genes (*Apaf-1* or *Casp3*) resulted in reduced apoptosis and recurrent brain malformations.<sup>32</sup> In this study, we found that rare variants in the *CASP9* gene were significantly more in human NTDs. Moreover, some of the identified missense variants impaired the protein's apoptotic function under complete or folate-deficient culture conditions.

In the p.Y251C variant, a tyrosine (which is absolutely conserved across all caspase-9 sequences analyzed) is changed to a cysteine in the catalytic domain of the protein. The catalytic domain harbors the catalytic cysteine at position 287 in the amino acid sequence (Figure 1B),<sup>33</sup> and the p.Y251C variant is close to the catalytic cysteine. The tyrosine to cysteine change is not a conservative substitution, as tyrosine contains an aromatic side chain and cysteine has an aliphatic side chain. Importantly, the introduction of a cysteine at this position would promote the formation of disulfide bonds with cysteine at other positions. The *CASP9* protein is composed of 416 amino acids, of which 13 are cysteine. A newly introduced cysteine could combine with the catalytic cysteine or other cysteines in the protein, potentially affecting the function of the catalytic domain. This could result, in part, in damage

to the catalytic activity or a loss of function. However, this mutation was found in 10 subjects (2 Hispanic, 7 European, and 1 South Asian) among 120,826 alleles in the ExAC database, and no association with diseases was found. This may be explained by its partially weakened efficiency to induce apoptosis.

It is generally known that women with low folate intake during pregnancy have significantly increased risk of carrying a fetus with NTDs.<sup>4</sup> Folate deficiency-induced reductions in proliferation and promotion of apoptosis have been verified in some cell lines and are related to neurological development and neurodegenerative diseases.<sup>34-36</sup> A recent study showed that mere folate deficiency did not induce NTDs in WT mouse embryos, whereas folate deficiency significantly increased NTDs in *spotch* (*Sp<sup>2H</sup>*) mutant litters, indicating a gene-environment interactions in the process of NTD formation.<sup>37</sup> Our data showed that p.R191G does not affect apoptosis compared with the WT under complete culture conditions, but it can reduce apoptosis compared with the WT in folate-deficient condition, implying that in conditions of folate insufficiency, the p.R191G variant potentially rescues abnormal apoptosis induced by malnutrition. Similar to the p.R191G variant, the p.Y251C variant exhibited reduced apoptotic function in low FA condition, which may be due to the production of an unstable protein. In this cohort, brain tissue folate concentrations of some cases carried the p.R191G variant, and case carried the p.Y251C variant was lower. Based on our present data, we speculate that the p.R191G and



p.Y251C variants potentially play a beneficial role in folate deficiency-induced NTDs. However, determination of the mechanisms underlying the effects of the p.R191G variant on apoptosis in folate deficiency, and the p.Y251C variant on the impairment of apoptosis, requires further study.

In contrast to *Casp9*<sup>-/-</sup> mice in which the NTD phenotype is localized to the midbrain and hindbrain, patients with *CASP9* missense variants exhibited cranial NTDs only in 2 cases; the other 5 cases presented with spinal defect phenotypes (Table 2). It has been reported that inhibition of apoptosis using the caspase inhibitor, Zvad-fmk, produces spinal NTDs in chicken embryos,<sup>38</sup> suggesting that inhibition of apoptosis can also influence spinal phenotype. NTD cases who carried *CASP9* gene mutations may have carried mutations of other NTDs candidate genes, which contributed to the production of cranial NTDs. Recently, 2 new aspects of the role of apoptosis in embryo neurulation were put forward: one is that apoptotic cells can affect tissue organization and shape by increasing the tension of surrounding cells in leg disk development and dorsal closure in *Drosophila* embryos<sup>31,39</sup>; the other is that apoptotic cells can eliminate FGF8 producing cells in the anterior neural ridge in mouse embryos, and a reduction in the number of apoptotic cells could lead to abnormal accumulation of FGF8 producing cells, thus disturbing gene expression and resulting in forebrain malformations.<sup>40</sup> Whether the mutations we identified have impacts on these 2 areas deserves further attention.

In summary, we have described rare mutations of the apoptosis gene *CASP9* identified in NTD cases and demonstrated that the p.Y251C variant impairs the protein's apoptotic function, suggesting it is a loss-of-function variation. We also showed that the p.R191G variant inhibited apoptosis under folate-deficient condition. Taken together, our findings confirm the association of apoptosis with human NTDs and highlight the effect of gene-environment interactions in this complex disease.

## ACKNOWLEDGEMENTS

This study was supported by the National Nature Science Foundation of China (Nos. 81771584, 81471163, and 81701441), the National Science & Technology Pillar Program during the 12th 5-year Plan Period (No. 2013BAI12B00), and CAMS Initiative for Innovative Medicine (No. CAMS-I2M-1-008).

## CONFLICT OF INTEREST

The authors declare no conflict of interest.

## ORCID

Ting Zhang  <http://orcid.org/0000-0002-6100-8327>

## REFERENCES

- Bassuk AG, Kibar Z. Genetic basis of neural tube defects. *Semin Pediatr Neurol*. 2009;16:101-110.
- Greene ND, Stanier P, Copp AJ. Genetics of human neural tube defects. *Hum Mol Genet*. 2009;18:R113-R129.
- Berry RJ, Li Z, Erickson JD, et al. Prevention of neural-tube defects with folic acid in China. China-U.S. collaborative project for neural tube defect prevention. *N Engl J Med*. 1999;341:1485-1490.
- Blom HJ, Shaw GM, den Heijer M, Finnell RH. Neural tube defects and folate: case far from closed. *Nat Rev Neurosci*. 2006;7:724-731.
- Chen S, Zhang Q, Bai B, et al. MARK2/Par1b insufficiency attenuates DVL gene transcription via histone deacetylation in lumbosacral spina bifida. *Mol Neurobiol*. 2017;54:6304-6316.
- Zhang T, Xin R, Gu X, et al. Maternal serum vitamin B12, folate and homocysteine and the risk of neural tube defects in the offspring in a high-risk area of China. *Public Health Nutr*. 2009;12:680-686.
- Harris MJ, Juriloff DM. An update to the list of mouse mutants with neural tube closure defects and advances toward a complete genetic perspective of neural tube closure. *Birth Defects Res A Clin Mol Teratol*. 2010;88:653-669.
- Yamaguchi Y, Shinotsuka N, Nonomura K, et al. Live imaging of apoptosis in a novel transgenic mouse highlights its role in neural tube closure. *J Cell Biol*. 2011;195:1047-1060.
- Kohlbecker A, Lee AE, Schorle H. Exencephaly in a subset of animals heterozygous for AP-2alpha mutation. *Teratol*. 2002;65:213-218.
- Ruland J, Duncan GS, Elia A, et al. Bcl10 is a positive regulator of antigen receptor-induced activation of NF-kappaB and neural tube closure. *Cell*. 2001;104:33-42.
- Riedl SJ, Shi Y. Molecular mechanisms of caspase regulation during apoptosis. *Nat Rev Mol Cell Biol*. 2004;5:897-907.
- Wurstle ML, Laussmann MA, Rehm M. The central role of initiator caspase-9 in apoptosis signal transduction and the regulation of its activation and activity on the apoptosome. *Exp Cell Res*. 2012;318:1213-1220.
- Hakem R, Hakem A, Duncan GS, et al. Differential requirement for caspase 9 in apoptotic pathways in vivo. *Cell*. 1998;94:339-352.
- Kuida K, Zheng TS, Na S, et al. Decreased apoptosis in the brain and premature lethality in CPP32-deficient mice. *Nature*. 1996;384:368-372.
- Kuida K, Haydar TF, Kuan CY, et al. Reduced apoptosis and cytochrome c-mediated caspase activation in mice lacking caspase 9. *Cell*. 1998;94:325-337.
- Leonard JR, Klocke BJ, D'Sa C, Flavell RA, Roth KA. Strain-dependent neurodevelopmental abnormalities in caspase-3-deficient mice. *J Neuropathol Exp Neurol*. 2002;61:673-677.
- Cecconi F, Alvarez-Bolado G, Meyer BI, Roth KA, Gruss P. Apaf1 (CED-4 homolog) regulates programmed cell death in mammalian development. *Cell*. 1998;94:727-737.
- Yoshida H, Kong YY, Yoshida R, et al. Apaf1 is required for mitochondrial pathways of apoptosis and brain development. *Cell*. 1998;94:739-750.
- Urase K, Kouroku Y, Fujita E, Momoi T. Region of caspase-3 activation and programmed cell death in the early development of the mouse forebrain. *Brain Res Dev Brain Res*. 2003;145:241-248.
- Hao Z, Duncan GS, Chang CC, et al. Specific ablation of the apoptotic functions of cytochrome C reveals a differential requirement for cytochrome C and Apaf-1 in apoptosis. *Cell*. 2005;121:579-591.
- Gangwar R, Mandhani A, Mittal RD. Caspase 9 and caspase 8 gene polymorphisms and susceptibility to bladder cancer in north Indian population. *Ann Surg Oncol*. 2009;16:2028-2034.
- Liamarkopoulos E, Gazouli M, Aravantinos G, et al. Caspase 8 and caspase 9 gene polymorphisms and susceptibility to gastric cancer. *Gastric Cancer*. 2011;14:317-321.
- Park JY, Park JM, Jang JS, et al. Caspase 9 promoter polymorphisms and risk of primary lung cancer. *Hum Mol Genet*. 2006;15:1963-1971.
- Theodoropoulos GE, Gazouli M, Vaiopoulou A, et al. Polymorphisms of caspase 8 and caspase 9 gene and colorectal cancer susceptibility and prognosis. *Int J Colorectal Dis*. 2011;26:1113-1118.
- Price RJ, Lillycrop KA, Burdge GC. Folic acid induces cell type-specific changes in the transcriptome of breast cancer cell lines: a proof-of-concept study. *J Nutr Sci*. 2016;5:e17.

26. Sdek P, Ying H, Chang DL, et al. MDM2 promotes proteasome-dependent ubiquitin-independent degradation of retinoblastoma protein. *Mol Cell*. 2005;20:699-708.
27. Reed JC, Doctor KS, Godzik A The domains of apoptosis: a genomics perspective. *Sci STKE*. 2004;2004: re9.
28. Schlett K, Madarasz E. Retinoic acid induced neural differentiation in a neuroectodermal cell line immortalized by p53 deficiency. *J Neurosci Res*. 1997;47:405-415.
29. Demeter K, Herberth B, Duda E, et al. Fate of cloned embryonic neuroectodermal cells implanted into the adult, newborn and embryonic forebrain. *Exp Neurol*. 2004;188:254-267.
30. Gu X, Lin L, Zheng X, et al. High prevalence of NTDs in Shanxi province: a combined epidemiological approach. *Birth Defects Res A Clin Mol Teratol*. 2007;79:702-707.
31. Toyama Y, Peralta XG, Wells AR, Kiehart DP, Edwards GS. Apoptotic force and tissue dynamics during *Drosophila* embryogenesis. *Science*. 2008;321:1683-1686.
32. Yamaguchi Y, Miura M. Programmed cell death in neurodevelopment. *Dev Cell*. 2015;32:478-490.
33. Srinivasula SM, Hegde R, Saleh A, et al. A conserved XIAP-interaction motif in caspase-9 and Smac/DIABLO regulates caspase activity and apoptosis. *Nature*. 2001;410:112-116.
34. Liang Y, Li Y, Li Z, et al. Mechanism of folate deficiency-induced apoptosis in mouse embryonic stem cells: cell cycle arrest/apoptosis in G1/G0 mediated by microRNA-302a and tumor suppressor gene *Lats2*. *Int J Biochem Cell Biol*. 2012;44:1750-1760.
35. Yang Y, Li X, Sun Q, et al. Folate deprivation induces cell cycle arrest at G0/G1 phase and apoptosis in hippocampal neuron cells through down-regulation of IGF-1 signaling pathway. *Int J Biochem Cell Biol*. 2016;79:222-230.
36. Zhang XM, Huang GW, Tian ZH, Ren DL, J XW. Folate deficiency induces neural stem cell apoptosis by increasing homocysteine in vitro. *J Clin Biochem Nutr*. 2009;45:14-19.
37. Burren KA, Savery D, Massa V, et al. Gene-environment interactions in the causation of neural tube defects: folate deficiency increases susceptibility conferred by loss of Pax3 function. *Hum Mol Genet*. 2008;17:3675-3685.
38. Weil M, Jacobson MD, Raff MC. Is programmed cell death required for neural tube closure? *Curr Biol*. 1997;7:281-284.
39. Monier B, Gettings M, Gay G, et al. Apico-basal forces exerted by apoptotic cells drive epithelium folding. *Nature*. 2015;518:245-248.
40. Nonomura K, Yamaguchi Y, Hamachi M, et al. Local apoptosis modulates early mammalian brain development through the elimination of morphogen-producing cells. *Dev Cell*. 2013;27:621-634.

**How to cite this article:** Liu X-Z, Zhang Q, Jiang Q, et al. Genetic screening and functional analysis of *CASP9* mutations in a Chinese cohort with neural tube defects. *CNS Neurosci Ther*. 2018;24:394-403. <https://doi.org/10.1111/cns.12797>